MODERN MATHEMATICAL METHODS
4 (2026), No. 1, pp. 50-68
https://modernmathmeth.com/
ISSN 3023 - 5294

Research Article

Approximation with rational and rescaled kernels: New steps forward

Dedicated to Professor Ioan Raşa, on the occasion of his 75th birthday

STEFANO DE MARCHI* AND ELISABETH LARSSON

ABSTRACT. The aim of this paper is to present new insights into Rational Radial Basis Function (RRBF) approximations and their localized rescaled counterparts. After some necessary notation, we briefly recall the essence of stable computational techniques for overcoming the ill-conditioning of the kernel matrices, as well as the ones that explore stable bases. RRBFs are then introduced, and their benefits are described. We discuss Variably Scaled Kernels, which provide a more flexible tool for approximating with RBFs, substituting the shape parameter with a scaling function. This scaling function is then applied to the RRBFs to obtain a new family of RBFs that are more appropriate for discontinuous functions. Finally, the localized version of the RRBFs is recalled, for which we provide new insights into an open conjecture regarding the sum of the cardinal function associated with the approximant in rescaled form.

Keywords: Radial basis function (RBF), variably scaled kernel, rational approximation, rescaled localized RBF.

2020 Mathematics Subject Classification: 41A20, 65D12, 65D15.

1. INTRODUCTION

Radial Basis Functions or RBF are functions that depend only on the Euclidean distance from a center point, i.e., $\phi(\|x-c\|)$, where x is a point in a given multidimensional domain and c is the center. Common RBFs include Gaussian, multiquadric, inverse multiquadric, and polyharmonic splines. They can be globally supported, locally supported, with different smoothness properties. Among the fundamental references, we recall these books [22, 24, 64].

Suppose we wish to conduct a literature search on platforms such as Google Scholar or specialized academic databases (e.g., IEEE Xplore, SpringerLink, or Elsevier's ScienceDirect). In that case, we can identify several thousand papers on RBFs across these fields. For example, a Google Scholar search for Radial Basis Functions yields more than 10^6 papers, including applications in machine learning, numerical analysis, and applied mathematics.

We can approximate functions or data at scattered points in $\mathbb{R}^M, M \geq 1$ by the following setting: Let $\Omega \subseteq \mathbb{R}^M$ be a bounded set, let $\mathcal{X}_N = \{\boldsymbol{x}_i, i = 1, \ldots, N\} \subseteq \Omega$ be a set of distinct data points (also called data sites or nodes) and let $\mathcal{F}_N = \{f_i = f(\boldsymbol{x}_i), i = 1, \ldots, N\}$ be a set of data values (or measurements or function values). The approximation problem consists in finding a function $P_f : \Omega \longrightarrow \mathbb{R}$ such that $P_f(\boldsymbol{x}_i) \approx f_i, i = 1, \ldots, N$. When equality holds we talk about interpolation. To this end, we consider $P_f \in \text{span}\{\Phi(\cdot, \boldsymbol{x}_i), \boldsymbol{x}_i \in \mathcal{X}_N\}$, where $\Phi : \Omega \times \Omega \longrightarrow \mathbb{R}$ is a strictly positive definite and symmetric kernel, for which the associated interpolation matrix A with entries $A_{i,j} = \Phi(x_i, x_j)$ is strictly positive definite. The interpolant then assumes the

Received: 06.03.2026; Accepted: 07.04.2026; Published Online: 15.04.2026
*Corresponding author: Stefano De Marchi; stefano.demarchi@unipd.it
DOI: 10.64700/mmm.119

form

$$P_f(\boldsymbol{x}) = \sum_{k=1}^{N} \alpha_k \Phi(\boldsymbol{x}, \boldsymbol{x}_k), \quad \boldsymbol{x} \in \Omega. \tag{1.1}$$

The coefficients $\boldsymbol{\alpha} = (\alpha_1, \ldots, \alpha_N)^T$ in (1.1) are found by solving the linear system $A\boldsymbol{\alpha} = \boldsymbol{f}$, with $\boldsymbol{f} = (f_1, \ldots, f_N)^T$, where A being strictly positive definite and symmetric ensures the uniqueness of the solution.

Definition 1.1. *A function $\sigma : \mathbb{R}^M \to \mathbb{R}$ is called radial, if there exists a continuous function $\phi : [0, \infty) \to \mathbb{R}$ such that $\sigma(\boldsymbol{x}) = \phi(r)$ with $r = \|\boldsymbol{x}\|_2$.*

Using this definition, given a basic function ϕ and the (symmetric positive definite) kernel Φ, for all $\boldsymbol{x}, \boldsymbol{y} \in \mathbb{R}^M$ we have a radial kernel just by considering $\Phi(\boldsymbol{x}, \boldsymbol{y}) = \phi(\|\boldsymbol{x} - \boldsymbol{y}\|_2)$. We can then indifferently use Φ or ϕ by referring to Definition 1.1. An example of a RBF is the well-known Gaussian function $\phi(r) = \mathrm{e}^{-\varepsilon^2 r^2}$, where ε is the shape parameter, which is indeed a scale parameter.

Many papers focus on using RBFs for the numerical solution of PDEs within a meshless framework. These methods include RBF collocation (cf. e.g. [9, 34, 41, 42]), RBF-generated finite differences (RBF-FD) (cf. e.g. [2, 25, 58, 59, 60]), and RBF partition of unity methods (RBF-PUM) (cf. e.g. [17, 38, 46]) with applications to elliptic, parabolic, and hyperbolic PDEs (especially in fluid dynamics, electromagnetics, and material science) (cf. e.g. [3, 5, 61, 63, 69]), option problems in the financial market [46, 57]. A significant portion of the research focuses on the use of RBFs for function interpolation and data fitting, which is fundamental to scattered data approximation. In machine learning, RBFs are used as kernels in algorithms like Support Vector Machines (SVMs) and in neural networks (Radial Basis Function Networks - RBFNs) (cf. e.g. [31, 43, 56]). These applications contribute to the large number of papers on RBFs in pattern recognition, classification, and regression. A large body of theoretical work deals with the analysis of convergence rates, error estimates, and the properties of different types of RBFs (e.g., Gaussian, multiquadric, inverse multiquadric) (see e.g. [10, 11, 12, 29, 39, 45, 49, 50, 51, 52, 54, 55, 65, 66, 67, 68]).

It is well-known that rational approximation (by using the ratio of polynomials) is more robust than the standard polynomial interpolation, in particular for functions characterized by steep gradients. However, this is a mesh-dependent approach and, as a consequence, extending polynomial approximation to higher dimensions is always quite hard (see, e.g., [32]). Moreover, there are many challenging issues associated with rational approximation, such as the computational cost (the number of coefficients to be determined is large) and the need to avoid singularities in the denominator (in higher dimensions, these are curves or manifolds).

In this paper, we would like to deepen the rescaled localized RBF approach, firstly used in [19] for the solution of PDEs with a meshless approach with compactly supported radial functions (see also [15, 16]), which represents a particular instance of rational RBFs (cf. [18, 33]).

The paper is organized as follows. In Section 2, we present preliminaries on stability and error analysis for RBFs. In Section 3, we recall some stable computational techniques, introduce Rational RBF, Variably Scaled Kernels and show that mixing them we can get a more stable approximation. In Section 4, we discussed the so-called Rescaled Localized RBF and presented new results on an open problem concerning the sum of the cardinals in this framework. We make some conclusions in Section 5.

2. Preliminaries on Stability and Error Analysis

It is well known that the ℓ_2 conditioning of a positive definite matrix K can be expressed

$$\text{cond}(\mathsf{K}) = \frac{\lambda_{\max}}{\lambda_{\min}}, \tag{2.2}$$

where $\lambda_{\max}, \lambda_{\min}$ are the largest and smallest eigenvalues of K respectively.

Remark 2.1. *The definition of ℓ_2 conditioning in (2.2) is valid as long as we deal with a square normal matrix K, i.e., it commutes with its conjugate transpose K^{H}. Such a definition is a particular case of the following formulation*

$$cond(\mathsf{A}) = \frac{\sigma_{\max}}{\sigma_{\min}},$$

which is true for any square matrix A. Here, $\sigma_{\max}$, $\sigma_{\min}$ are the largest and smallest singular values of A respectively.

Concerning the largest eigenvalue, if K is the $N \times N$ positive definite kernel matrix related to a translational invariant kernel $\Phi(\boldsymbol{x}, \boldsymbol{y}) = \phi(\boldsymbol{x} - \boldsymbol{y})$, an immediate consequence of Gershgorin's theorem is that

$$\lambda_{\max} \leq N\phi(\mathbf{0}).$$

For error analysis, we sometimes need the approximant to be expressed in terms of cardinal functions (cf. [22, Section 14.2]).

Theorem 2.1. *Let $\Omega \subset \mathbb{R}^d$ and let Φ be a strictly positive definite kernel. Then, for every set $X = \{\boldsymbol{x}_k,\ k = 1, \ldots, N\} \subset \Omega$ of distinct node points there exist functions $u_k^* \in span\{\Phi(\cdot, \boldsymbol{x}_k),\ k = 1, \ldots, N\}$ such that $u_i^*(\boldsymbol{x}_j) = \delta_{ij}$, where δ_{ij} is the well-known Kronecker delta.*

By means of the so-defined functions u_k^*, $k = 1, \ldots, N$, also called cardinal functions, we can write the interpolant in (1.1) of a given function $f : \Omega \longrightarrow \mathbb{R}$ in its Lagrangian form [71], that is,

$$P_f(\boldsymbol{x}) = \sum_{k=1}^{N} f(\boldsymbol{x}_k)\, u_k^*(\boldsymbol{x}), \quad \boldsymbol{x} \in \Omega. \tag{2.3}$$

Let $\Phi \in \mathcal{C}(\Omega \times \Omega)$. For any set of distinct nodes X_N and vector $\boldsymbol{u} \in \mathbb{R}^N$ we can consider the quadratic form

$$Q(\boldsymbol{u}) := \Phi(\boldsymbol{x}, \boldsymbol{x}) - 2\sum_{k=1}^{N} u_k \Phi(\boldsymbol{x}, \boldsymbol{x}_k) + \sum_{i=1}^{N}\sum_{j=1}^{N} u_i u_j \Phi(\boldsymbol{x}_i, \boldsymbol{x}_j).$$

Then, we give the following definition [22, Section 14.3].

Definition 2.2. *Let $\Omega \subseteq \mathbb{R}^d$ and let $\Phi \in C(\Omega \times \Omega)$ be a strictly positive definite kernel. Then, for any set of distinct points $X = \{\boldsymbol{x}_k,\ k = 1, \ldots, N\} \subseteq \Omega$ we define the power function*

$$[P_{X,\Phi}(\boldsymbol{x})]^2 := Q(\boldsymbol{u}^*(\boldsymbol{x})),$$

where $\boldsymbol{u}^*$ is the vector of cardinal functions (see Theorem 2.1).

The power function can also be computed as

$$P_{X,\Phi}(\boldsymbol{x}) = \sqrt{\Phi(\boldsymbol{x}, \boldsymbol{x}) - (\boldsymbol{b}(\boldsymbol{x}))^{\mathsf{T}}\, \mathsf{K}^{-1} \boldsymbol{b}(\boldsymbol{x})},$$

where $\boldsymbol{b} = (\Phi(\cdot, \boldsymbol{x}_1), \ldots, \Phi(\cdot, \boldsymbol{x}_N))^\intercal$ and K is the kernel matrix defined previously. Moreover, letting $\mathsf{K}^{\boldsymbol{y}}$ be the kernel matrix related to the augmented dataset $X \cup \{\boldsymbol{y}\}$, we can also express the power function as (see [13])

$$P_{X,\Phi}(\boldsymbol{y}) = \sqrt{\frac{\det \mathsf{K}^{\boldsymbol{y}}}{\det \mathsf{K}}}. \tag{2.4}$$

Remark 2.2. *The power function vanishes if it is evaluated at the interpolation nodes, as emphasized by the formulation in* (2.4).

Thanks to the power function definition, we can now provide the following error bound for the kernel-based interpolant in (2.3) [22, Section 14.4].

Theorem 2.2. *Let $\Omega \subseteq \mathbb{R}^d$ and let $\Phi \in \mathcal{C}(\Omega \times \Omega)$ be a strictly positive definite kernel. Moreover, let $X = \{\boldsymbol{x}_k, k = 1, \ldots, N\} \subset \Omega$ be a set of distinct nodes. Then*

$$|f(\boldsymbol{x}) - P_f(\boldsymbol{x})| \leq P_{X,\Phi}(\boldsymbol{x}) \|f\|_{\mathcal{N}_\Phi(\Omega)}, \quad \boldsymbol{x} \in \Omega,$$

where $f \in \mathcal{N}_\Phi(\Omega)$.

Despite the dependency on the power function, and thus on the chosen set of nodes, we observe that Theorem 2.2 provides a pointwise error bound that does not give any indication concerning the mesh size, a term used in abuse of notation in the scattered data interpolation context. To obtain further details in this direction, we introduce the so-called separation distance and the fill distance [22, Section 14.1].

Definition 2.3. *The separation distance is defined as*

$$q_X := \frac{1}{2} \min_{i \neq j} \|\boldsymbol{x}_i - \boldsymbol{x}_j\|.$$

Definition 2.4. *The fill distance is given by*

$$h_{X,\Omega} := \sup_{\boldsymbol{x} \in \Omega} \min_{\boldsymbol{x}_k \in X} \|\boldsymbol{x} - \boldsymbol{x}_k\|.$$

Remark 2.3. *Geometrically, the quantity q_X represents the radius of the largest ball that can be centered at every point in X so that there is no overlap. At the same time, $h_{X,\Omega}$ is the radius of the largest empty ball that can be placed among the data sites in Ω.*

3. Stable Computation Techniques

One of the most investigated topics is the behaviour of the kernel interpolant in the *flat* limit, i.e., when $\varepsilon \longrightarrow 0$ (cf. e.g. [20, 36, 39, 53]) and associated methods for stable evaluation of the kernel interpolant in the limit (cf. e.g. [26, 70]). In agreement with the trade-off principles [50], we remark the following:

- In some cases, the approximants may suffer from instability because of the ill-conditioning of the interpolation matrices as the shape parameter becomes small, corresponding to the so-called flat RBFs [26]. This problem depends on both the smoothness order of the basis function and the node distribution. More specifically, if one keeps the number of nodes fixed and considers smooth basis functions, then the problem of instability becomes evident for small values of the shape parameter.
- A radial basis function with a finite order of smoothness can be used to improve the conditioning, but the accuracy of the fit gets worse. For this reason, recent research has moved towards the study of stable bases (see e.g. [14, 23, 27, 28]).

Among the most popular methods for stabilizing the interpolant, many belong to the following categories.

(1) **RBF-QR Method**. It is rooted in a particular decomposition of the kernel, and it has been developed so far to treat the Gaussian kernel [23, 27, 28, 35].
(2) **Hilbert-Schmidt Singular Value Decomposition (HS-SVD)**. It has been developed to stably compute the RBF interpolants [8, 24]. In principle, this technique can be applied to any kernel, provided that the HS eigenvalues and eigenvectors are known. However, these quantities are far from being easy to compute, and in practice, they only work for the Gaussian function.
(3) **WSVD Bases**. It is a more general approach that applies to any RBF, consisting of computing a weighted SVD decomposition which produces stable bases [14].

3.1. **Rational Radial Basis Functions (RRBFs).** Aiming to modify the kernel basis to improve computational stability, we here present a recent research topic which develop rational RBF approximation. We start by recalling the main theoretical and computational aspects studied in [6]. The method reported here is the so-called eigen-rational kernel-based scheme. It consists of a fractional RBF expansion, with the denominator depending on the eigenvector associated to the largest eigenvalue of the kernel matrix.

We have already seen that the spaces spanned by kernels provide beneficial properties for multivariate approximation. Nevertheless, it might be advantageous to study approximants in non-linear spaces generated by RBFs. A few examples of these approaches already exist in the literature and are known as rational RBFs, introduced in [33] and further developed in [16, 47]. The main disadvantage of the scheme proposed in these papers is that the rational basis is constructed from function values, and consequently, it depends not only on the data sites. A solution comes from the eigen-rational basis.

We recall that rational real functions are expressed as ratios of polynomials. That is, at each point $x \in \mathbb{R}$

$$R(x) = \frac{P_n(x)}{Q_m(x)} = \frac{a_n x^n + a_{n-1}x^{n-1} + \cdots a_1 x + a_0}{b_m x^m + b_{m-1}x^{m-1} + \cdots b_1 x + b_0}\,.$$

The collection $\{a_n, a_{n-1}, \ldots, a_0; b_m, b_{m-1}, \ldots, b_0\}$ is the set of the coefficients of R, that can be computed imposing some interpolation conditions. It is also usually assumed that the polynomials P_n and Q_m are relatively prime, that is, common factors are canceled.

Rational RBFs (RRBFs) are an extension of classical radial basis functions (RBFs) that, starting from two RBF approximations, say R_1, R_2 expressed as in (1.1), can be similarly expressed as the ratio of them. It has proven to be an effective tool for solving both interpolation problems and partial differential equations (PDEs) (cf. e.g. [6, 16]).

Fix the integers m, n, k and j so that $m, n \le N$, $1 \le k \le N + m - 1$ and $1 \le j \le N + n - 1$. Letting $\mathcal{X}_m = \{\boldsymbol{x}_i, i = k, \ldots, k+m-1\}$ and $\mathcal{X}_n = \{\boldsymbol{x}_i, i = j, \ldots, j+n-1\}$ two non-empty subsets of $\mathcal{X}_N \subseteq \Omega (\subseteq \mathbb{R}^M)$, a natural extension of the classical RBF approximation to the rational case, is then

$$\mathscr{R}(\boldsymbol{x}) = \frac{R^{(1)}(\boldsymbol{x})}{R^{(2)}(\boldsymbol{x})} = \frac{\sum_{i_1=k}^{k+m-1} \alpha_{i_1} \Phi(\boldsymbol{x}, \boldsymbol{x}_{i_1})}{\sum_{i_2=j}^{j+n-1} \beta_{i_2} \Phi(\boldsymbol{x}, \boldsymbol{x}_{i_2})}, \tag{3.5}$$

provided $R^{(2)}(\boldsymbol{x}) \neq 0$, $\boldsymbol{x} \in \Omega$. Details concerning the well-posedness and the solution of the interpolation problem, as well as the error analysis, can be found in [16, 33]. In particular, the well-posedness as discussed in [16, §3.2] for $n = m = N$, is equivalent to finding the eigenvector, say $\mathbf{q}$, associated with the smallest eigenvalue in modulus of a generalized eigenvalue

problem:

$$\Lambda \boldsymbol{q} = \lambda \Theta \boldsymbol{q},$$

with

$$\Lambda = \frac{1}{||\boldsymbol{f}||_2^2} D^T A^{-1} D + A^{-1}, \quad \text{and} \quad \Theta = \frac{1}{||\boldsymbol{f}||_2^2} D^T D + I_N,$$

where I_N is the $N \times N$ identity matrix, A is the kernel matrix defined above and $D = \texttt{diag}(f_1, \ldots, f_n)$. Hence, we have to simply define $\mathcal{R}^{(1)}$ and $\mathcal{R}^{(2)}$ as standard RBF interpolants of $\boldsymbol{p}$ and $\boldsymbol{q}$, respectively. Some known benefits of using Rational RBFs:

- **Improved Stability**. Rational RBFs are significantly more accurate than standard RBFs for functions with steep gradients or discontinuous behavior, both in the neighborhood of the discontinuity and away from it and for solving PDEs with such solutions (cf. [47]). Moreover, when using flat, infinitely smooth kernels (like Gaussians), which are desirable for high accuracy but cause severe ill-conditioning, rational RBF methods can be implemented in a stable manner (e.g., using Variably Scaled Kernels or RBF-QR), preventing the system matrix from becoming overly unstable (cf.[16, 37]).
- **Multiscale Behavior**. Rational RBFs can handle multiscale phenomena, which are common in many PDE problems (e.g., fluid dynamics, wave propagation) (cf. e.g. [62]).
- **Boundary Conditions**. Rational RBFs can better handle boundary conditions in PDEs by providing more accurate approximations near the boundaries of the domain (cf. [21]).

3.2. **Variably Scaled Kernels.** This subsection briefly describes an interesting approach to the shape parameter issues, called Variably Scaled Kernels, shortly VSK. We recall the definition as in [4, Definition 2.1].

Definition 3.5. *Let $\Phi : \mathbb{R}^{(d+1)\times(d+1)} \longrightarrow \mathbb{R}$ be a continuous strictly positive definite radial kernel and let $\psi : \mathbb{R}^d \longrightarrow \mathbb{R}$ be a scaling function. A variably scaled kernel Φ^Ψ on $\mathbb{R}^{d\times d}$ is defined as*

$$\Phi^\Psi(\boldsymbol{x}, \boldsymbol{y}) = \Phi((\boldsymbol{x}, \psi(\boldsymbol{x})), (\boldsymbol{y}, \psi(\boldsymbol{y}))), \tag{3.6}$$

for $\boldsymbol{x}, \boldsymbol{y} \in \mathbb{R}^d$.

We note that the shape parameter of the underlying kernel Φ in Definition 3.5 is chosen equal to 1. We do not include this information in the notation for simplicity and to avoid overly complicated notation.

Remark 3.4. *Often we consider radial kernels: the VSK for radial kernels becomes*

$$\Phi^\Psi(\boldsymbol{x}, \boldsymbol{y}) = \phi\left(\sqrt{\|\boldsymbol{x} - \boldsymbol{y}\|^2 + |\psi(\boldsymbol{x}) - \psi(\boldsymbol{y})|^2}\right),$$

where ϕ is the usual univariate function related to Φ. In other words, if Φ is radial on $\mathbb{R}^{(d+1)\times(d+1)}$ so is Φ^Ψ on $\mathbb{R}^{d\times d}$. Moreover, if Φ is (strictly) positive definite, so is Φ^Ψ.

By considering the map $\Psi(\boldsymbol{x}) = (\boldsymbol{x}, \psi(\boldsymbol{x}))$ on Ω and in analogy with (1.1), we can express the VSK interpolant at the nodes $\tilde{X} = \{(\boldsymbol{x}_k, \psi(\boldsymbol{x}_k)),\ \boldsymbol{x}_k \in X\}$ as

$$R(\Psi(\boldsymbol{x})) = \sum_{k=1}^{N} c_k \Phi(\Psi(\boldsymbol{x}), \Psi(\boldsymbol{x}_k)), \tag{3.7}$$

with $\boldsymbol{x} \in \Omega,\ \boldsymbol{x}_k \in X$. Therefore, in order to obtain a VSK interpolant R^Ψ at the set of nodes X on Ω, it is sufficient to project back the interpolant in (3.7), that is,

$$R^\Psi(\boldsymbol{x}) = \sum_{k=1}^{N} c_k \Phi^\Psi(\boldsymbol{x}, \boldsymbol{x}_k) = \sum_{k=1}^{N} c_k \Phi(\Psi(\boldsymbol{x}), \Psi(\boldsymbol{x}_k)) = R(\Psi(\boldsymbol{x})).$$

An important consequence of this construction is that the analysis of the variably scaled setting is fully understood in terms of the analysis of the underlying standard kernel (which is composed with Ψ). The following proposition in [4] states some additional properties of VSKs, which are fundamental to understanding why VSKs improve the stability of the approximation process.

Proposition 3.1. *Let Φ, Φ^Ψ, and ψ be as in Definition 3.5. We have*

(i) If Φ and ψ are continuous, so is Φ^Ψ. Moreover, if $\psi : \Omega \to \psi(\Omega)$ is a bijection, then Φ^ψ inherits the positiveness properties of Φ.

(ii) Let q_X be the separation distance between the centers (see Definition 2.3 above), we have

$$q_X \leq q_{\Psi(X)}$$

for any choice of the scaling map ψ. Indeed, by the definition of the Euclidean norm, we have

$$\|\Psi(\boldsymbol{x}_i) - \Psi(\boldsymbol{x}_j)\|^2 = \|\boldsymbol{x}_i^2 - \boldsymbol{x}_j^2\|^2 + (\psi(\boldsymbol{x}_i) - \psi(\boldsymbol{x}_j))^2 \leq \|\boldsymbol{x}_i^2 - \boldsymbol{x}_j^2\|^2 (1+L)^2,$$

where L is the Lipschitz constant of ψ.

(iii) Let $G_\Psi(\Omega) = \{(\boldsymbol{x}, \psi(\boldsymbol{x})) \mid \boldsymbol{x} \in \Omega\} \subset \Omega \times \mathbb{R}$ be the graph of the scaling function ψ. Then, the native spaces $\mathcal{N}_\Phi(G_\Psi(\Omega))$ and $\mathcal{N}_{\Phi^\Psi}(\Omega)$ are isometrically isomorphic (cf. [4, Theorem 2]*).*

Remark 3.5. *As a consequence of Proposition 3.1 (ii), the variably scaled setting might improve the stability of the interpolation process by increasing the separation distance.*

Remark 3.6. *The interpolation via Variably Scaled Kernels (VSKs) depends on the definition of an appropriate scaling function, but no fixed theoretical or numerical recipes for its construction have been provided. Recently, in* [1]*, a user-independent tool for learning the scaling function using Discontinuous Neural Networks (called δ-NN) was presented, which partially addresses this gap.*

3.3. **Rational Kernel-Based Approximation.** In [6], an eigen-rational kernel-based scheme was proposed for multivariate interpolation using meshfree methods. Let us suppose that $\Phi : \mathbb{R}^d \times \mathbb{R}^d \to \mathbb{R}$ is a conditionally positive definite kernel and $\bar{\Phi}$ its associate positive definite one (for example, Φ can be a generalized multiquadrics of order 2, $\bar{\Phi}$ is the inverse multiquadrics). We note that if Φ is strictly positive definite, we set $\hat{\Phi} = \Phi$ so that we use the same kernel matrix for both the numerator and the denominator (for example, consider Φ as the Matérn kernel). We can define the interpolant of a function f

$$\hat{P}_f(\boldsymbol{x}) = \frac{\sum_{i=1}^{N} \alpha_i \Phi(\boldsymbol{x}, \boldsymbol{x_i}) + \sum_{m=1}^{L} \gamma_m p_m(\boldsymbol{x})}{\sum_{k=1}^{N} \beta_k \bar{\Phi}(\boldsymbol{x}, \boldsymbol{x_k})} = \frac{P_g(\boldsymbol{x})}{P_h(\boldsymbol{x})}, \tag{3.8}$$

defined for some function values g_i, h_i, $i = 1, \ldots, N$. Roughly speaking, once we provide the function values h_i, we can construct P_g in the standard way, i.e., such that it interpolates $\boldsymbol{g} = (f_1 h_1, \ldots, f_N h_N)^\intercal$. Then, obviously, $\hat{P}_f$ interpolates the given function values $\mathcal{F}_N$ at the nodes $\mathcal{X}_N$. This definition, for the one given above in (3.5), for constructing P_g, adapts the more general case of conditionally positive definite kernels, still restricting to the case of strictly positive kernels for P_h. This enables us to make the eigen-rational interpolant well-defined, i.e. such that $P_h(\boldsymbol{x}) \neq 0$, for all $\boldsymbol{x} \in \Omega$. We recall that a similar approach for the class of

polyharmonic kernels considered both in the numerator and denominator of (3.8), has been investigated in [21].

Proposition 3.2. *The method consists of a fractional RBF expansion, with the denominator depending on the largest eigenvalue of the kernel matrix.*

Proof. We need to define $\hat{P}_f$ by using the cardinal functions, $\hat{u}_j$ (which form a partition of unity) (cf. [6, Theorem 2.3]). If the kernel $\bar{K}$ is strictly positive definite, the same argument holds for functions $\bar{u}_k \in \text{span}\{\bar{K}(\cdot, \boldsymbol{x}_j), \quad j = 1, \ldots, N\}$. Therefore,

$$P_g(\boldsymbol{x}) = \sum_{k=1}^{N} g(\boldsymbol{x}_k)\, u_k(\boldsymbol{x}), \quad P_h(\boldsymbol{x}) = \sum_{k=1}^{N} h(\boldsymbol{x}_k)\, \bar{u}_k(\boldsymbol{x}), \quad \boldsymbol{x} \in \Omega.$$

Thus, the resulting eigen-rational interpolant in cardinal form is given by

$$\begin{aligned}\hat{P}_f(\boldsymbol{x}) =& \frac{\sum_{j=1}^{N} g_j u_j(\boldsymbol{x})}{\sum_{k=1}^{N} h_k \bar{u}_k(\boldsymbol{x})} = \frac{\sum_{j=1}^{N} h_j f_j u_j(\boldsymbol{x})}{\sum_{k=1}^{N} h_k \bar{u}_k(\boldsymbol{x})} \\ =& \sum_{j=1}^{N} f_j \frac{h_j u_j(\boldsymbol{x})}{\sum_{k=1}^{N} h_k \bar{u}_k(\boldsymbol{x})} =: \sum_{j=1}^{N} f_j \hat{u}_j(\boldsymbol{x}),\end{aligned}$$

and, furthermore, $\hat{u}_i(\boldsymbol{x}_i) = \delta_{ik}$, $\boldsymbol{x}_i \in \mathcal{X}_N$. Moreover, if $K = \bar{K}$ is strictly positive definite, $\{\hat{u}_j\}_{j=1}^{N}$ form a partition of unity. Indeed for $\boldsymbol{x} \in \Omega$

$$\sum_{j=1}^{N} \hat{u}_j(\boldsymbol{x}) = \sum_{j=1}^{N} h_j \frac{\bar{u}_j(\boldsymbol{x})}{\sum_{k=1}^{N} h_k \bar{u}_k(\boldsymbol{x})} = \frac{\sum_{j=1}^{N} h_j \bar{u}_j(\boldsymbol{x})}{\sum_{k=1}^{N} h_k \bar{u}_k(\boldsymbol{x})} = 1.$$

Considering

$$\sum_{j=1}^{N} (\hat{u}_j(\boldsymbol{x}))^2 = \sum_{j=1}^{N} \left(\frac{h_j u_j(\boldsymbol{x})}{\sum_{k=1}^{N} h_k \bar{u}_k(\boldsymbol{x})} \right)^2 \leq \frac{||\boldsymbol{h}^2||_\infty}{P_h^2(\boldsymbol{x})} \sum_{j=1}^{N} (u_j(\boldsymbol{x}))^2,$$

and from [64, Theorem 12.1, p. 208], we know that

$$1 + \sum_{j=1}^{N} (u_j(\boldsymbol{x}))^2 \leq \frac{\mathcal{P}_{K,\mathcal{X}_N}^2(\boldsymbol{x})}{\omega}, \tag{3.9}$$

where ω is the smallest eigenvalue of the kernel matrix constructed on the node set $\mathcal{X}_N \cup \{\boldsymbol{x}\}$ with $\omega > 0$. This concludes the proof. □

This also provides an upper bound for the Lebesgue function $\sum_{j=1}^{N} |\hat{u}_j|$. Classical bounds in terms of Lebesgue constants and convergence rates with respect to the mesh size of the eigen-rational interpolant showed to be comparable with the ones of the classical kernel-based methods, as discussed in [6].

3.4. **Variably Scaled Rational Kernels (VSRK).** Both strategies, Rational RBF plus VSK, can be combined to form a new family of kernels, which we denote as Variably Scaled Rational Kernels (VSRK). The idea is to take advantage of the flexibility of the VSK and their stability properties, which, combined with those of the rational kernels, can yield even better approximation results. At the moment, we have not developed a complete analysis of these claims (it will appear in a forthcoming paper). In fact, the variably scaled kernel injects strictly positive spectral mass, preventing eigenvalues from collapsing to zero, which directly improves conditioning and therefore stability. Let $X = \{x_1, \ldots, x_N\} \subset \mathbb{R}^d$, $K_r : X \times X \to \mathbb{R}$ be a rational

positive definite kernel, and $K_s : X \times X \to \mathbb{R}$ be a variably scaled positive definite kernel. Define the combined kernel:

$$K_\gamma(x,y) := K_r(x,y) + \gamma K_s(x,y), \quad \gamma > 0.$$

Theorem 3.3. *Let $\mathbf{K}_r, \mathbf{K}_s, \mathbf{K}_\gamma \in \mathbb{R}^{N\times N}$ be the corresponding kernel matrices. If $\mathbf{K}_s$ is strictly positive definite, then $\mathbf{K}_\gamma$ is strictly positive definite, and we have*

$$\lambda_{\min}(\mathbf{K}_\lambda) \geq \lambda_{\min}(\mathbf{K}_r) + \gamma\lambda_{\min}(\mathbf{K}_s), \tag{3.10}$$

$$\kappa(\mathbf{K}_\gamma) \leq \frac{\lambda_{\max}(\mathbf{K}_r) + \gamma\lambda_{\max}(\mathbf{K}_s)}{\lambda_{\min}(\mathbf{K}_r) + \gamma\lambda_{\min}(\mathbf{K}_s)}. \tag{3.11}$$

Proof. The proof goes as follows:

(1) **Positive Definiteness.** Since K_r and K_s are positive definite kernels, their matrices satisfy: $\mathbf{K}_r \succeq 0, \quad \mathbf{K}_s \succ 0$. For any nonzero vector $c \in \mathbb{R}^N$, $c^T\mathbf{K}_\gamma c = c^T\mathbf{K}_r c + \gamma c^T\mathbf{K}_s c$. Because $c^T\mathbf{K}_r c \geq 0$ and $c^T\mathbf{K}_s c > 0$, it follows that $c^T\mathbf{K}_\gamma c > 0$, hence $\mathbf{K}_\gamma \succ 0$.

(2) **Lower Bound on Eigenvalues.** By Weyl's inequality for symmetric matrices, that is $\lambda_{\min}(\mathbf{A}+\mathbf{B}) \geq \lambda_{\min}(\mathbf{A}) + \lambda_{\min}(\mathbf{B})$, and applying this to $\mathbf{K}_r$ and $\gamma\mathbf{K}_s$, we get formula (3.10)

$$\lambda_{\min}(\mathbf{K}_\gamma) \geq \lambda_{\min}(\mathbf{K}_r) + \gamma\lambda_{\min}(\mathbf{K}_s).$$

(3) **Upper Bound on Eigenvalues.** Similarly,

$$\lambda_{\max}(\mathbf{K}_\gamma) \leq \lambda_{\max}(\mathbf{K}_r) + \gamma\lambda_{\max}(\mathbf{K}_s).$$

(4) **Condition Number Bound.** By definition, $\kappa(\mathbf{K}_\gamma) = \frac{\lambda_{\max}(\mathbf{K}_\lambda)}{\lambda_{\min}(\mathbf{K}_\lambda)}$. Hence, by using the bounds above,

$$\kappa(\mathbf{K}_\gamma) \leq \frac{\lambda_{\max}(\mathbf{K}_r) + \gamma\lambda_{\max}(\mathbf{K}_s)}{\lambda_{\min}(\mathbf{K}_r) + \gamma\lambda_{\min}(\mathbf{K}_s)}.$$

(5) **Stability Improvement.** If $\lambda_{\min}(\mathbf{K}_r)$ is small (ill-conditioning), then the denominator is increased by $\gamma\lambda_{\min}(\mathbf{K}_s) > 0$, leading to a reduced condition number and improved numerical stability.

This concludes the proof. □

Remark 3.7. *If, instead, one defines*

$$K(x,y) = K_r(x,y)K_s(x,y), \tag{3.12}$$

then the corresponding kernel matrix is the Hadamard product $\mathbf{K} = \mathbf{K}_r \circ \mathbf{K}_s$. By the Schur product theorem, $\mathbf{K}$ is positive definite. Moreover, under mild assumptions,

$$\lambda_{\min}(\mathbf{K}) \geq \min_i(\mathbf{K}_s)_{ii}\ \lambda_{\min}(\mathbf{K}_r)$$

showing that K_s acts as a local preconditioner improving stability.

Here, we provide a couple of examples that demonstrate the effectiveness of the new approach. In both examples, we consider the centers to be a set X_c of $N = 81$ Halton points, and the evaluation points to be the set X_e of $M = 100$ equally spaced points. Moreover, we consider $\hat{\Phi} = \Phi$, in particular we take the C^6 Matérn kernel. The Rational+VSK interpolant is obtained by evaluating the rational interpolant $\hat{P}_f$ whose coefficients are constructed by solving linear systems with matrices constructed at the sets $\psi(X_c)$ and $\psi(X_e)$.

Here, we outline the algorithm for constructing the VSRK interpolant.

(1) Given the function Φ, ψ and f the sets of the centers, C and the evaluation points, E. Consider $C_\psi = (C, \psi(C)), E_\psi = (E, \psi(E))$. Let $B1$ and $B2$ be the corresponding kernel matrices
(2) Find, for instance with the power method, the eigenvector $\tilde{x}$ corresponding to maximum eigenvalue of the matrix $B2$, and set $a = B\tilde{x}$
(3) Let $p = f\ \tilde{x}$, where $f_i = f(\boldsymbol{c}_i)$ with $\boldsymbol{c}_i$ the $i-th$ center
(4) Find the coefficients $\boldsymbol{\alpha}$ of the interpolant by solving the linear system $B1\ \boldsymbol{\alpha} = p$
(5) Hence, the VSRK interpolant is

$$\hat{P}_f^\psi = \frac{E\boldsymbol{\alpha}}{E\hat{x}}$$

with E the kernel matrix at the evaluation points mapped by ψ.

Example 3.1. *The first numerical example consists of the function*

$$f(x) = \begin{cases} \sin(x) + \cos(x), & x \geq \pi/4 \\ \sqrt{2}, & 0 \leq x < \pi/4 \end{cases} . \tag{3.13}$$

This is a continuous function that we approximate using a C^6 Matérn rational VSK kernel with $\psi(x) = 2\log(x)/\pi$. The function ψ and the resulting plot of f and the comparison with the rational approximant $\hat{P}_f$ and $\hat{P}_f$+VSK are displayed in Fig. 1.

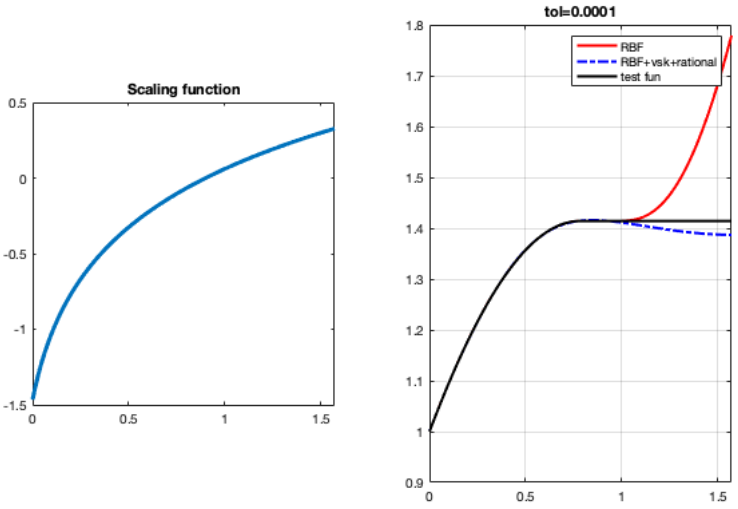

FIGURE 1. Left: The scaling function. Right: The function (3.13), the approximation with classical rational and the rational+VSK

Example 3.2. *The second numerical example consists of a function*

$$f(x) = \begin{cases} 0.4 + x^8/\tan(1+x^2) + 0.5, & x > 1/2 \\ \sin(x), & 0 \leq x \leq 1/2 \end{cases} . \tag{3.14}$$

This is a discontinuous function that we approximate using a Matérn rational discontinuous VSK kernel with

$$\psi(x) = \begin{cases} 1, & x > 1/2 \\ -1, & 0 \leq x \leq 1/2 \end{cases} .$$

The results are displayed in Fig. 2.

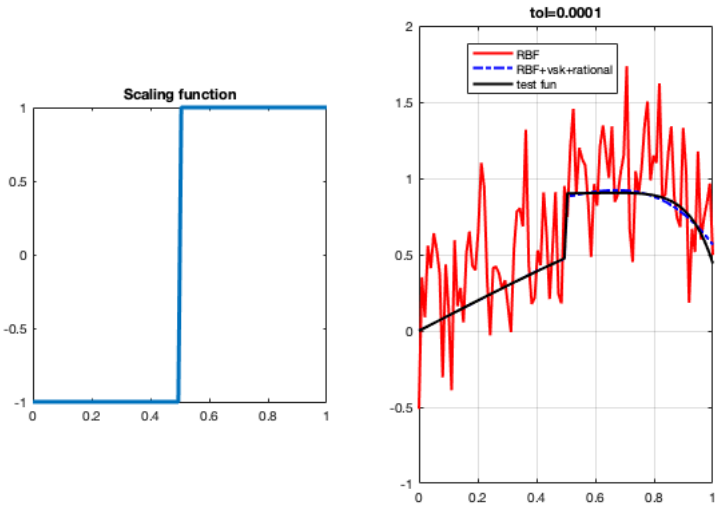

FIGURE 2. Left: The scaling function. Right: The function (3.14), the approximation with classical rational and the rational+VSK

4. RESCALED LOCALIZED RBFS

The idea of the RL-RBF, introduced in [19], is that of computing the RBF interpolant of a function f, based on a compactly supported ϕ, that we call P_f, and the interpolant of the constant function $g \equiv 1$, say P_1, and form their quotient. The new approximation $\hat{P}_f$ is then

$$\hat{P}_f := \frac{P_f}{P_1}. \tag{4.15}$$

The Rescaled Localized Radial Basis Function (RL-RBF) interpolant is then a simple rational approximation method (see e.g. [15, 18]). The construction simply goes as follows.

Let $\mathcal{X}_N = \{\boldsymbol{x}_1, \ldots, \boldsymbol{x}_N\} \subset \Omega \subset \mathbb{R}^d$ and consider two functions $f, g : \mathbb{R}^d \to \mathbb{R}$, s.t. $g(\mathbb{R}^d) = 1$ and consider the function

$$\hat{\mathcal{P}}_f(\mathcal{X}_N; \boldsymbol{x}) = \frac{\mathcal{P}_f(\mathcal{X}_N; \boldsymbol{x})}{\mathcal{P}_g(\mathcal{X}_N; \boldsymbol{x})}$$

where $\mathcal{P}_\cdot(\mathcal{X}_N; \boldsymbol{x})$ is a standard, generic RBF interpolant. We notice that $\hat{\mathcal{P}}_f(\mathcal{X}_N; \boldsymbol{x})$ is still an interpolant to f, since

$$\hat{\mathcal{P}}_f(\mathcal{X}_N; \mathcal{X}_N) = \frac{\mathcal{P}_f(\mathcal{X}_N; \mathcal{X}_N)}{\mathcal{P}_g(\mathcal{X}_N; \mathcal{X}_N)} = \frac{f(\mathcal{X}_N)}{g(\mathcal{X}_N)} = f(\mathcal{X}_N).$$

Heuristically, it has been showed in [15, 19] that

- $\hat{\mathcal{P}}_f$ is powerful when compactly supported RBF are chosen.
- If ϵ is the shape parameter, there exists $\hat{\epsilon}$ and $(\hat{\epsilon} - \delta_1, \hat{\epsilon} + \delta_2)$ s.t. if ϵ stands in the left side, $\hat{\mathcal{P}}_f$ behaves better than $\mathcal{P}_f$, while on the right side it shows the opposite.
- $\hat{\mathcal{P}}_f$ is, in general, much less sensitive to the setting of ϵ than $\mathcal{P}_f$.
- $\hat{\mathcal{P}}_f$ can be not defined if $\mathcal{X}_N$ doesn't have a sufficiently homogeneous density in Ω.

About the associated native space, we recall the classical result from functional analysis.

Theorem 4.4 (Aronszajn). *Let $K : \Omega \times \Omega \to \mathbb{R}$ be a (strictly) positive definite kernel. Let $s : \Omega \to \mathbb{R}$ be a continuous and nonvanishing function on Ω. Then*

$$K_s(\boldsymbol{x}, \boldsymbol{y}) = s(\boldsymbol{x})s(\boldsymbol{y})K(\boldsymbol{x}, \boldsymbol{y})$$

is (strictly) positive definite.

Letting $s(\cdot) = \frac{1}{\mathcal{P}_g(\mathcal{X}_N, \cdot)}$, if $\mathcal{X}_N$ is s.t. $\mathcal{P}_g(\Omega) \neq 0$, then

$$K_r(\boldsymbol{x}, \boldsymbol{y}) = \frac{1}{\mathcal{P}_g(\mathcal{X}_N, \boldsymbol{x})} \frac{1}{\mathcal{P}_g(\mathcal{X}_N, \boldsymbol{y})} K(\boldsymbol{x}, \boldsymbol{y})$$

is a kernel, and by considering the usual inner product, we can build the associated Native Space $\mathcal{N}_{K_r}$. Furthermore, let $\{u_j(\boldsymbol{x}_i) = \delta_{i,j}\}_j$ be the cardinals for $\mathcal{P}_f$,

$$\hat{\mathcal{P}}_f(\mathcal{X}_N, \boldsymbol{x}) = \frac{\sum_{j=1}^N f(\boldsymbol{x}_j)u_j}{\sum_{k=1}^N u_k} = \sum_{j=1}^N f(\boldsymbol{x}_j) \frac{u_j}{\sum_{k=1}^N u_k}$$

leads to a natural definition of $\frac{u_j}{\sum_{k=1}^N u_k} := \hat{u}_j$.

Theorem 4.5. *The rescaled interpolation method is a Shepard's method, where the weight functions are defined as $\hat{u}_j = u_j / \left(\sum_{k=1}^N u_k\right)$, $\{u_j\}_j$ being the cardinal basis of span$\{K(\cdot, x), x \in X\}$.*

The Lebesgue function and constant are, then,

$$\hat{\Lambda}_N(\boldsymbol{x}) := \sum_{j=1}^N |\hat{u}_j(\boldsymbol{x})|, \quad \hat{\lambda}_N := \|\hat{\Lambda}_N\|_{\infty,\Omega}$$

that gives an estimate for the stability,

$$\|\hat{P}_f\|_{\infty,\Omega} \leq \hat{\lambda}_N \|f\|_{\infty,X}.$$

A comparison of the Lebesgue constants is given in Figure 3.

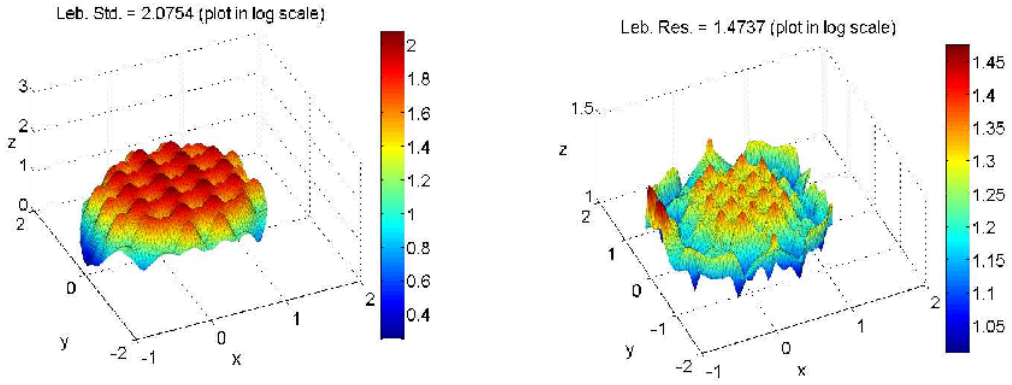

FIGURE 3. Standard basis (Left) and rescaled one (Right), $\mathcal{C}^2$ Wendland kernel on the square, $\varepsilon = 3.85$

In [18], the convergence of the RL-RBF method in the case of quasi-uniform data and stationary scaling has been discussed. As the method is not only interpolatory but also reproduces constants exactly (in fact, it is equivalent to the Shepard's method), linear convergence is expected. We showed that this linear convergence holds up to a certain conjecture about the sum of the rescaled cardinal functions. Concerning the convergence, the following Lemma posed an *open problem* on the sum of the cardinals.

Lemma 4.1. *Under the assumptions of* [18, Theorem 2.3], *there is a constant* $c > 0$ *such that*

$$\sum_{j=1}^{N} u_j(\boldsymbol{x}) \geq c, \qquad \boldsymbol{x} \in \Omega. \tag{4.16}$$

Remark 4.8. *Unfortunately, this Lemma has not been proved. One can easily check, by resorting to the fact that each cardinal is a ratio of two strictly positive determinants (similarly to the Lagrange elementary functions in the polynomial case), that it holds for* $n = 2$. *For* $n > 2$, *in* [18] *it was extensively checked by many numerical examples, even in the case of standard approximation, and in all cases it was confirmed. In Figure 4, we report the numerical results obtained from stable computations using the RBF-QR method for the Gaussian RBF.*

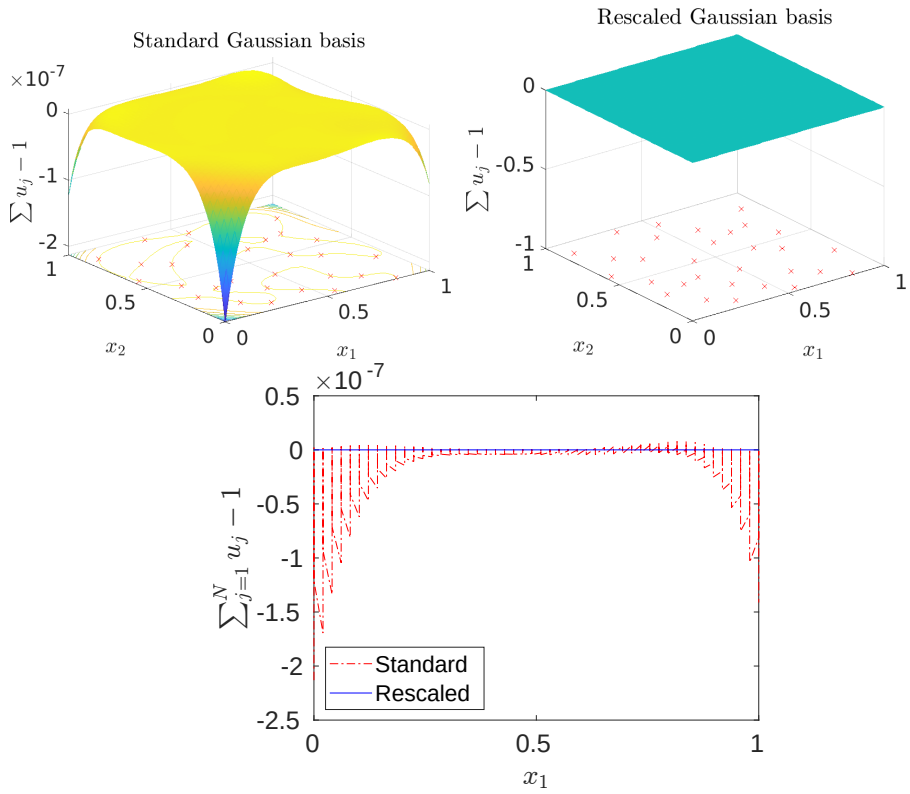

FIGURE 4. RBF-QR. Sum of the cardinals on a grid 50×50 centered at 30 Halton points: Standard, rescaled, and the comparison of their 1-d profiles, for the Gaussian function with $\varepsilon = \sqrt{2}/4$

4.1. **The Case of the Gaussian.** In the forthcoming publication [40], it is shown that for small enough values of the shape parameter ε, and for a unisolvent node set $X = \{\boldsymbol{x}_i\}_{i=1}^N$ in d dimensions, the Gaussian interpolant $s(x,\varepsilon)$ to the data vector $f(X)$ can be expressed on the following closed form that is not ill-conditioned as a function of the shape parameter

$$s(\boldsymbol{x},\varepsilon) = P_K(\boldsymbol{x}) + (Q(\boldsymbol{x},X) - vV^{-1}Q(X,X))(I + Q(X,X))^{-1}f(X), \tag{4.17}$$

where P_K is the unique interpolation polynomial of degree K, which means that $N = \binom{K+d}{d}$, V is the (multivariate) Vandermonde matrix for the given nodes, and v is a row vector evaluating the monomial basis at an arbitrary point $\boldsymbol{x}$. For the details of the function Q, we refer to [40]. When the data $f(X)$ is sampled from a polynomial of degree $\leq K$, the interpolation polynomial $P_K(\boldsymbol{x})$ is the exact solution and the second term in (4.17) is the interpolation error. In particular, if the data is constant, such that $f_0(X) \equiv 1$, then the error is given by

$$E_0(\boldsymbol{x},\varepsilon) = (Q(\boldsymbol{x},X) - vV^{-1}Q(X,X))(I + Q(X,X))^{-1}f_0(X). \tag{4.18}$$

We note that the first factor is the polynomial interpolation error of Q, and we also note that the second factor alternatively can be expressed as the power series $I - Q + Q^2 - \cdots$.

4.1.1. *Error in the 1-d Case.* A detailed analysis of the full error expression has been performed for the 1-d case. When the shape parameter $\varepsilon \lesssim 1$, $\|Q\| < 1$ and the second factor can be approximated by I. Hence, we focus on the interpolation error of $Q(x,X)f_0(X)$. By analyzing the leading order terms of Qf_0 and using the standard error estimate for 1-d polynomial interpolation, we find the approximate error to be

$$E_0(x,\varepsilon) \approx \frac{\prod_{i=0}^K (x - x_i)}{(K+1)!} \frac{\varepsilon^{2\lfloor \frac{K+2}{2} \rfloor}}{(\lfloor \frac{K+2}{2} \rfloor)!}. \tag{4.19}$$

The analytical error estimate is compared with the actual errors in Figure 5, showing excellent agreement across the different types of node sets and numbers of points tested.

The estimate (4.19) illustrates the separation of the dependence of the error on the nodes and on the shape parameter. A large fill distance h due to an uneven node distribution increases the error, and uniform nodes lead to a larger error at the boundary, especially for large K, just as for polynomial interpolation in general. For interpolation of a constant (or other monomials of degree $\leq K$), the error decreases towards zero as an even power of the shape parameter.

In the detailed analysis of Q, we find that it is beneficial for the approximation to have nodes symmetric about the origin. In the experiments that are shown in Figure 5, all node sets are scaled to cover the full interval [-1,1]. The uniform and Chebyshev nodes are symmetric, while the Halton nodes are not.

The theoretical estimate as well as the numerical results show that for Gaussian RBFs in 1-d, we can provide sufficient conditions on the number of nodes, the distribution of nodes, and the shape parameter ε, such that Lemma 4.1 is satisfied for a given c, showing that the RL-RBF method is well defined and has at least linear convergence in this case.

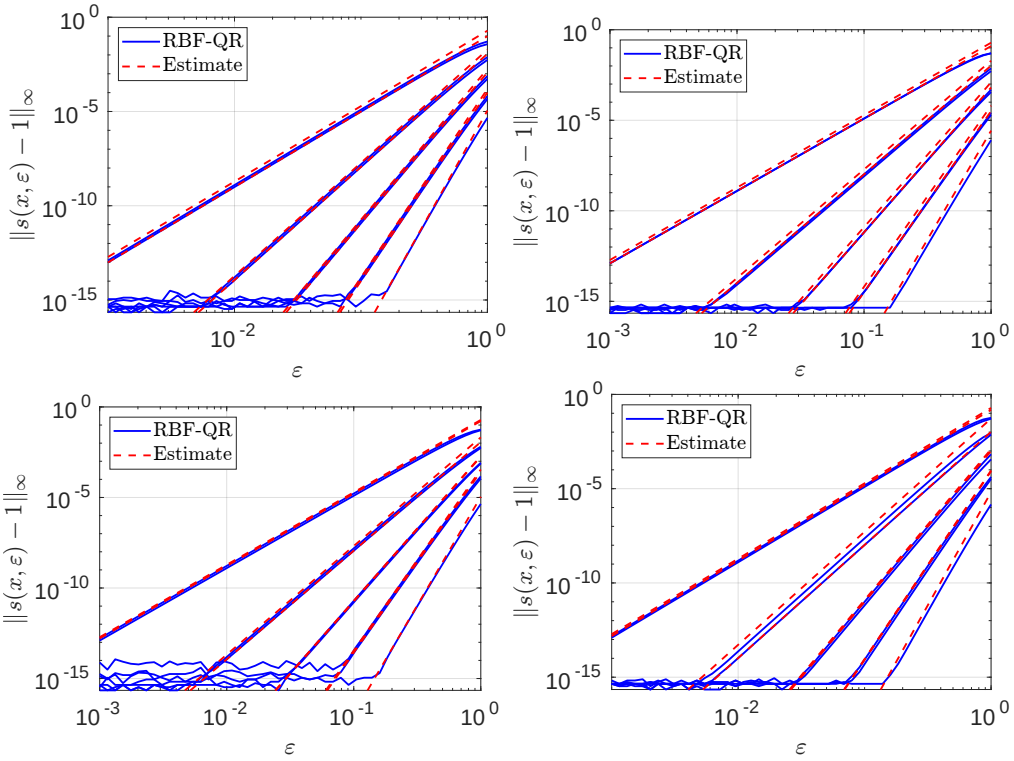

FIGURE 5. The actual Gaussian interpolation errors computed using the RBF-QR method and the error approximation (4.19) for constant data. The node points used were uniform (top left), Chebyshev (top right), Halton (bottom left), and Halton nodes clustered toward the boundary (bottom right) for polynomial degrees $K = 2, \ldots, 10$. Note that curves for $K = 2s$ and $K = 2s+1$ are similar in all plots and can be hard to distinguish

5. CONCLUSION AND FUTURE WORK

In this paper, we present new insights into rational RBFs and their simple counterparts for compactly supported RBFs that reproduce constant functions, denoted Rescaled Localized RBFs. We have also presented a new error estimate for the Gaussians that splits into two parts: one depending on the choice of nodes and the other on the shape parameter. This allows, at least in 1-d, to provide sufficient conditions for the well-definedness of the RL-RBF and its linear convergence.

As future work, we observe that polynomial reproduction plays a relevant role in deriving error estimates for various approximation schemes. Local reproduction in a quasi-uniform setting is a significant factor in error estimation and stability assessment, but for some computationally relevant schemes, such as the RL-RBF, it becomes a limitation. To facilitate the study of a wider range of approximation methods in a unified and efficient manner, a framework based on fast-decaying polynomial reproduction has been proposed in the master's thesis [7]. That is, we do not restrict the method to using compactly supported basis functions, but we instead allow the basis functions to decay to infinity as a function of the separation distance.

The implementation of fast-decaying polynomial reproduction yields stable, convergent methods that are smooth when approximated by moving least squares or very efficient for linear programming problems.

Acknowledgments

This research has been supported by the *Knut and Alice Wallenberg Foundation*, Visiting Professor program 2025, grant no. KAW 2024.0300. The first author also acknowledges the INdAM-GNCS group and the topical group on Approximation Theory and Applications of the Italian Mathematical Union. The second author also acknowledges the Swedish Research Council, grant no. 2016-04849.

Appendix A. Matlab Code

This is the core of the Matlab code for the Variably Scaled Rational Kernel.

```
dsites1 = [dsites psi(dsites,b)];
epoints1 = [epoints psi(epoints,b)];
ctrs1 = dsites1;
DM_data = DistanceMatrix(dsites1,ctrs1);
DM_eval = DistanceMatrix(epoints1,ctrs1);

IM1 = rbf1(ep,DM_data);
B1=IM1+mu.*eye(N);
IM2 = rbf2(ep,DM_data);
B2=IM1+mu.*eye(N);
x0=ones(N,1);
[x1]= powermethod(x0,IM2,1e-6);
int=(B2*x1);
p = rhs.*x1; % Define the vector p
coef = [B1\(rhs.*int)  x1]; % solve linear system B*pAlpha = p
EM1 = rbf1(ep,DM_eval);
ap_rational_vsk=(EM1*coef(:,1))./(EM1*x1);
```

References

[1] G. Audone, F. Della Santa, E. Perracchione and S. Pieraccini: *A recipe for learning variably scaled kernels via discontinuous neural networks*, J. Comput. Appl. Math., **469** (2025), 1–18.

[2] V. Bayona, N. Flyer, B. Fornberg and G. A. Barnett: *On the role of polynomials in RBF-FD approximations: II. numerical solution of elliptic PDEs*, J. Comput. Phys., **332** (2017), 257–273.

[3] F. Bernal, A. Safdari-Vaighani and E. Larsson: *A radial basis function partition of unity method for steady flow simulations*, J. Comput. Phys., **503** (2024), Article ID:112842.

[4] M. Bozzini, L. Lenarduzzi, M. Rossini and R. Schaback: *Interpolation with variably scaled kernels*, IMA J. Numer. Anal., **35** (2015), 199–219.

[5] C. Bracco, O. Davydov, C. Giannelli and A. Sestini: *A positive meshless finite difference scheme for scalar conservation laws with adaptive artificial viscosity driven by fault detection*, Comput. Math. Appl., **190** (2025), 103–121.

[6] M. D. Buhmann, S. De Marchi and E. Perracchione: *Analysis of a new class of rational RBF expansions*, IMA J. Numer. Anal., **40** (3) (2020), 1972–1993.

[7] G. Cappellazzo: *Fast decaying polynomial reproduction*, Master's thesis, University of Padova, Padua (2023).

[8] R. Cavoretto, G. E. Fasshauer and M. McCourt: *An introduction to the Hilbert-Schmidt SVD using iterated Brownian bridge kernels*, Numer. Algorithms, **68** (2015), 393–422.

[9] C. S. Chen, A. Karageorghis and H. Zheng: *Improved RBF collocation methods for fourth order boundary value problems*, Commun. Comput. Phys., **27** (2020), 1530–1549.

[10] M. Chen, L. Ling and D. Yun: *Proving the stability estimates of variational least-squares kernel-based methods*, Comput. Math. Appl., **180** (2025), 46–60.

[11] O. Davydov, R. Schaback: *Error bounds for kernel-based numerical differentiation*, Numer. Math., **132** (2016), 243–269.

[12] O. Davydov, R. Schaback: *Optimal stencils in Sobolev spaces*, IMA J. Numer. Anal., **39** (2019), 398–422.

[13] S. De Marchi: *On optimal center locations for radial basis function interpolation: computational aspects*, Rend. Semin. Mat., Univ. Politec. Torino, **61** (2003), 343–358.

[14] S. De Marchi, G. Santin: *A new stable basis for radial basis function interpolation*, J. Comput. Appl. Math., **253** (2013), 1–13.

[15] S. De Marchi, A. Idda and G. Santin: *A rescaled method for RBF approximation*, Proceedings of Approximation Theory XV, Springer Proceedings on Mathematics and Statistics, **201**, San Antonio, Texas (USA) (2017), 39–59.

[16] S. De Marchi, A. Martínez and E. Perracchione: *Fast and stable rational RBF-based partition of unity interpolation*, J. Comput. Appl. Math., **349** (2019), 331–343.

[17] S. De Marchi, A. Martínez, E. Perracchione and M. Rossini: *RBF-based partition of unity methods for elliptic PDEs: Adaptivity and stability issues via variably scaled kernels*, J. Sci. Comput., **79** (2019), 321–344.

[18] S. De Marchi, H. Wendland: *On the Convergence of the rescaled localized radial basis function method*, Appl. Math. Letters, **99** (2020), Article ID:105996.

[19] S. Deparis, D. Forti and A. Quarteroni: *A rescaled localized radial basis function interpolation on non-cartesian and non-conforming grids*, SIAM J. Sci. Comp., **36** (6) (2014), A2745–A2762.

[20] T. A. Driscoll, B. Fornberg: *Interpolation in the limit of increasingly flat radial basis functions*, Comput. Math. Appl., **43** (2002), 413–422.

[21] E. Farazandeh, D. Mirzaei: *A rational RBF interpolation with conditionally positive definite kernels*, Adv. Comput. Math., **47** (2021), Article ID:74.

[22] G. E. Fasshauer: *Meshfree approximations methods with Matlab*, World Scientific, Singapore (2007).

[23] G. E. Fasshauer, M. J. McCourt: *Stable evaluation of Gaussian radial basis function interpolants*, SIAM J. Sci. Comput., **34** (2012), A737–A762.

[24] G. E. Fasshauer, M. J. McCourt: *Kernel-based approximation methods using Matlab*, World Scientific, Singapore (2015).

[25] N. Flyer, E. Lehto, S. Blaise, G. B. Wright and A. St-Cyr: *A guide to RBF-generated finite differences for nonlinear transport: shallow water simulations on a sphere*, J. Comput. Phys., **231** (2012), 4078–4095.

[26] B. Fornberg, G. Wright: *Stable computation of multiquadric interpolants for all values of the shape parameter*, Comput. Math. Appl., **48** (2004), pp. 853-867.

[27] B. Fornberg, C. Piret: *A stable algorithm for flat radial basis functions on a sphere*, SIAM J. Sci. Comput., **30** (2007), 60–80.

[28] B. Fornberg, E. Larsson and N. Flyer: *Stable computations with Gaussian radial basis functions*, SIAM J. Sci. Comput., **33** (2011), 869–892.

[29] T. Hangelbroek, F. J. Narcowich, C. Rieger and J. D. Ward: *An inverse theorem for compact Lipschitz regions in* $\mathbb{R}^d$ *using localized kernel bases*, Math. Comp., **87** (2018), 1949–1989.

[30] H. Harbrecht, M. Multerer: *Samplets: Construction and scattered data compression*, J. Comput. Physics, **471** (2022), Article ID:111616.

[31] T. Hofmann, B. Schölkopf and A. J. Smola: *Kernel methods in machine learning*, Ann. Statist., **36** (3) (2008), 1171–1220.

[32] X. G. Hu, T. S. Ho and H. Rabitz: *Rational approximation with multidimensional scattered data*, Phys. Rev., **65** (2002), Article ID:035701.

[33] S. Jakobsson, B. Andersson and F. Edelvik: *Rational radial basis function interpolation with applications to antenna design*, J. Comput. Appl. Math., **233** (2009), 889–904.

[34] E. J. Kansa: *Application of Hardy's multiquadric interpolation to hydrodynamics*, in: Proc. 1986 Simul. Conf., **4** (1986), 111–117.

[35] K. Kormann, C. Lasser and A. Yurova: *Stable interpolation with isotropic and anisotropic Gaussians using Hermite generating function*, SIAM J. Sci. Comput., **41** (2019), A3839–A3859.

[36] E. Larsson, B. Fornberg: *Theoretical and computational aspects of multivariate interpolation with increasingly flat radial basis functions*, Comput. Math. Appl., **49** (2005), 103–130.

[37] E. Larsson, E. Lehto, A. R. H. Heryudono and B. Fornberg: *Stable computation of differentiation matrices and scattered node stencils based on Gaussian radial basis functions*, SIAM J. Sci. Comput., **33** (2013), 869–892.

[38] E. Larsson, V. Shcherbakov and A. Heryudono: *A least squares radial basis function partition of unity method for solving PDEs*, SIAM J. Sci. Comput., **39** (2017), A2538–A2563.

[39] E. Larsson, R. Schaback: *Scaling of radial basis functions*, IMA J. Numer. Anal., **44** (2024), 1130–1152.

[40] E. Larsson: *On the optimal shape parameter of Gaussian radial basis function interpolation*, manuscript in preparation, (2026).

[41] X. Li, M. Chen, Z. Sun, L. Ling and S. Li: *Energy-conserving Kansa methods for Hamiltonian wave equations*, Appl. Math. Comput., **510** (2026), Article ID:129682.

[42] L. Ling, R. Opfer and R. Schaback: *Results on meshless collocation techniques*, Eng. Anal. Bound. Elem., **30** (2006), 247–253.
[43] M. J. L. Orr: *Introduction to radial basis function networks*, Tech. rep., Centre for Cognitive Sciences, University of Edinburgh, Edinburgh (1996).
[44] B. Raeisi, M. Fardi and M. A. Darani: *RBF-based partition of unity methods for two-dimensional time-dependent PDEs: Numerical and theoretical aspects*, Math. Comput. Simulation, **226** (2024), 152–171.
[45] C. Rieger, H. Wendland: *Constructive approximation of high-dimensional functions with small efficient dimension with applications in uncertainty quantification*, SIAM J. Numer. Anal., **64** (2026), 1–28.
[46] A. Safdari-Vaighani, A. Heryudono and E. Larsson: *A radial basis function partition of unity collocation method for convection-diffusion equations arising in financial applications*, J. Sci. Comput., **64** (2015), 341–367.
[47] S. Sarra: *A rational radial basis function method for accurately resolving discontinuities and steep gradients*, Appl. Math. Comput., **160** (2018), 131–142.
[48] S. Sarra: *Local radial basis function methods: Comparison, improvements and implementation*, J. Appl. Math. Phys., **11** (2023), 3867–3886.
[49] R. Schaback: *Lower bound for norms of inverses of interpolation matrices for radial basis functions*, J. Approx. Theory, **79** (1994), 287–306.
[50] R. Schaback: *Error estimates and condition numbers for radial basis function interpolation*, Adv. Comput. Math., **3** (1995), 251–264.
[51] R. Schaback: *Native Hilbert spaces for radial basis functions. I.*, In: New developments in approximation theory, **132**, Birkhäuser, Basel (1999), 255–282.
[52] R. Schaback: *A unified theory of radial basis functions: Native Hilbert spaces for radial basis functions II*, J. Comput. Appl. Math., **121** (2000), 165–177.
[53] R. Schaback: *Multivariate interpolation by polynomials and radial basis functions*, Constr. Approx., **21** (2005), 293–317.
[54] R. Schaback: *Convergence of unsymmetric kernel-based meshless collocation methods*, SIAM J. Numer. Anal., **45** (2007), 333–351.
[55] R. Schaback: *All well-posed problems have uniformly stable and convergent discretizations*, Numer. Math., **132** (2016), 597–630.
[56] B. Schölkopf, A. J. Smola: *Learning with kernels: Support vector machines, regularization, optimization, and beyond*, MIT Press, Cambridge (2002).
[57] V. Shcherbakov, E. Larsson: *Radial basis function partition of unity methods for pricing vanilla basket options*, Comput. Math. Appl., **71** (2016), 185–200.
[58] J. Slak, G. Kosec: *On generation of node distributions for meshless PDE discretizations*, SIAM J. Sci. Comput., **41** (2019), A3202–A3229.
[59] J. Slak, B. Stojanovič and G. Kosec: *High order RBF-FD approximations with application to a scattering problem*, 4th International Conference on Smart and Sustainable Technologies (SpliTech 2019), Split & Bol. (Croatia) (2019).
[60] I. Tominec, E. Larsson, and A. Heryudono: *A least squares radial basis function finite difference method with improved stability properties*, SIAM J. Sci. Comput., **43** (2021), A1441–A1471.
[61] I. Tominec, M. Nazarov and E. Larsson: *Stability estimates for radial basis function methods applied to linear scalar conservation laws*, Appl. Math. Comput., **485** (2025), Article ID:129020.
[62] Z. Wang, M. Chen and J. Chen: *Solving multiscale elliptic problems by sparse radial basis function neural networks*, J. Comput. Phys., **492** (2023), Article ID:112452.
[63] B.-S. Wang, A. S. L. Chu, L. Ling and W. S. Don: *Foliation structures and global flow dynamics of scalar hyperbolic conservation laws on manifolds: I. Geometry-compatible fluxes and numerical validation on sphere and torus*, Commun. Nonlinear Sci. Numer. Simul., **152** (2026), Article ID:109415.
[64] H. Wendland: *Scattered data approximation*, Cambridge Monogr. Appl. Comput. Math., **17**, Cambridge Univ. Press, Cambridge (2005).
[65] T. Wenzel, G. Santin and B. Haasdonk: *Stability of convergence rates: kernel interpolation on non-Lipschitz domains*, IMA J. Numer. Anal., **45** (2025), 777–798.
[66] T. Wenzel: *Sharp inverse statements for kernel interpolation*, Math. Comp., **95** (2026), 1389–1413.
[67] T. Wenzel, A. Iske: *Spectral equivalence of unsymmetric kernel matrices and applications*, BIT, **66** (2026), Article ID:14.
[68] T. Wenzel, G. Santin and B. Haasdonk: *Analysis of structured deep kernel networks*, J. Comput. Appl. Math., **476** (2026), Article ID:116975.
[69] A. Westermann, O. Davydov, A. Sokolov and S. Turek: *Stability and accuracy of a meshless finite difference method for the Stokes equations*, Internat. J. Numer. Methods Engrg., **126** (2025), Article ID:e70000.
[70] G. B. Wright, B. Fornberg: *Stable computations with flat radial basis functions using vector-valued rational approximations*, J. Comput. Phys., **331** (2017), 137–156.
[71] Z. Wu, R. Schaback: *Local error estimates for radial basis function interpolation of scattered data*, IMA J. Numer. Anal., **13** (1993), 13–27.

STEFANO DE MARCHI
UNIVERSITY OF PADOVA
DEPARTMENT OF MEDICINE
35128, PADUA, ITALY
SELÇUK UNIVERSITY
DEPARTMENT OF MATHEMATICS
SELÇUKLU, KONYA, TÜRKIYE
Email address: stefano.demarchi@unipd.it

ELISABETH LARSSON
UPPSALA UNIVERSITY
DEPARTMENT OF INFORMATION TECHNOLOGY
SE-751 05, UPPSALA, SWEDEN
Email address: elisabeth.larsson@it.uu.se